# Harmonically mode-locked Ti:Er:$LiNbO_3$ waveguide laser

**H. Suche, R. Wessel, S. Westenhöfer, and W. Sohler**

*Angewandte Physik, Universität-GH Paderborn, Warburgerstrasse 100, D-33098 Paderborn, Germany*

**S. Bosso, C. Carmannini, and R. Corsini**

*Divisione Italia, Direzione Ricerca e Sviluppo, Pirelli Cavi SpA, Viale Sarca 202, I-20126 Milano, Italy*

Received September 9, 1994

Active mode locking of an Er-diffusion-doped Ti:$LiNbO_3$ waveguide laser by intracavity phase modulation to as high as the fourth harmonic (5.12 GHz) of the axial-mode frequency spacing is reported. The diode-pumped, pigtailed, and fully packaged laser with a monolithically integrated intracavity phase modulator has a threshold of 9 mW (incident pump power $E_p \parallel c$) and emits transform-limited pulses of $\geq$3.8-ps width and $\leq$5.6-pJ pulse energy (gain-switched mode locking) at 1602-nm wavelength ($E_s \parallel c$). The relative change of the mode-locking frequency with the temperature is $3.65 \times 10^{-5}$/°C. The mode-locking acceptance bandwidth is $\pm$75 kHz near the axial-mode frequency spacing at approximately five times the threshold pump power.

Erbium diffusion doping of $LiNbO_3$ has allowed the development of—besides efficient integrated amplifiers—integrated optical lasers that can take advantage of both the excellent electro-optic and acousto-optic properties of the host and of the gain that the dopant yields near the 1.55-$\mu$m wavelength. The method of selective doping was developed to permit the monolithic integration of active and passive components on the same substrate.[1] Besides free-running waveguide lasers at various wavelengths,[2,3] the first mode-locked waveguide laser was recently demonstrated.[4] Mode locking was achieved by synchronous intracavity phase modulation (FM mode locking) of the resonant laser field with the axial-mode frequency spacing. In this Letter we report mode locking to as high as the fourth harmonic of the axial mode spacing of a diode-pumped fully packaged Er:Ti:$LiNbO_3$ waveguide laser. The mode-locked pulses have been investigated by use of the optical autocorrelation method.

The design of the laser with a monolithically integrated intracavity traveling-wave phase modulator is shown schematically in Fig. 1. Z-cut $LiNbO_3$ has been chosen owing to its higher diffusivity for $Er^{3+}$ ions normal to the surface.[1] 11 nm of sputtered Er was indiffused at 1100 °C for 100 h in an oxygen atmosphere, producing a Gaussian concentration profile of $\cong$5-$\mu$m $1/e$ penetration depth. Subsequently, channel waveguides were fabricated by standard Ti indiffusion of photolithographically defined 7-$\mu$m-wide 95-nm-thick Ti stripes. Using a distributed-feedback laser diode at 1548.9-nm wavelength, we measured a total waveguide attenuation (scattering losses and absorption) of 1.2 dB/cm (TE, $E \perp c$) and 1.1 dB/cm (TM, $E \parallel c$), with approximately 0.1 dB/cm owing to scattering losses in TE polarization. Mode intensity distributions (FWHM) at 1550 nm are 4.8 $\mu$m $\times$ 3.5 $\mu$m (width $\times$ depth) for TM and 6.8 $\mu$m $\times$ 4.5 $\mu$m for TE. The intracavity phase modulator has traveling-wave electrodes defined by photolithographic lift-off of an evaporated Au layer and subsequent electroplating. The measured serial resistance is $\cong$ 10 $\Omega$, and the calculated rf impedance, neglecting ohmic losses, is $\cong$ 45 $\Omega$. At low frequencies a half-wave voltage $V_\pi \cong 8$ V has been measured. We placed the modulator on top of the waveguide to utilize the largest electro-optic coefficient $r_{33}$ for phase modulation (Z-cut $LiNbO_3$). To prevent significant excess losses for TM modes, we coated the substrate with an insulating $SiO_2$ buffer layer before the electrode fabrication. A dielectric-mirror Fabry–Perot waveguide cavity was fabricated by reactive e-beam evaporation of alternating $SiO_2/TiO_2$ layers onto the polished waveguide end faces. The pump input mirror of the 54-mm-long cavity is designed as a low-pass filter of high transmittance at the pump wavelength ($\lambda_p \cong 1480$ nm) and, simultaneously, of high reflectance at the laser emission wavelengths (1602 nm TM, 1611 nm TE). The output coupler has a high reflectance at the laser emission wavelengths and at the pump wavelength, leading to a double-pass pumped configuration. We pigtailed the laser by using a standard (9/125-$\mu$m) single-mode fiber at the input and an oriented polarization-maintaining fiber (York HB 1500) at the output. Afterward, the pigtailed device was mounted on a Cu block, with a thermistor and a thermoelectric cooler for temperature stabilization, and then packaged in an Al housing.

To pump the Ti:Er:$LiNbO_3$ waveguide laser, we used a pigtailed diode laser[5] near 1475 nm [width of spectral power density, 15 nm (FWHM)] connected to the pump input fiber. The mode-locked laser output has been separated from the transmitted pump by use of a wavelength-division demultiplexer. The oriented polarization-maintaining output fiber permitted us to identify unambiguously the polarization of the waveguide laser emission.

At a pump power level of 9 mW [$\pi$ (TM) polarized], TM-polarized lasing at 1602 nm set in. The

0146-9592/95/060596-03$6.00/0 

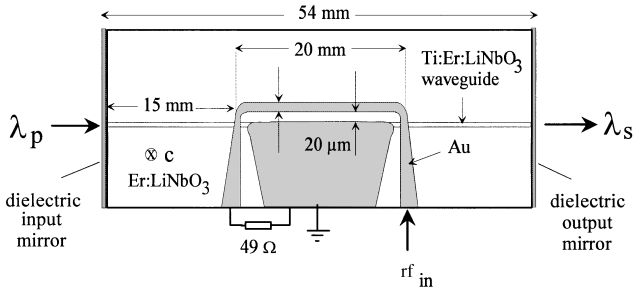


Fig. 1. Schematic of the dielectric-mirror Ti:Er:$LiNbO_3$ waveguide laser with a monolithically integrated intracavity traveling-wave phase modulator (mode locker).

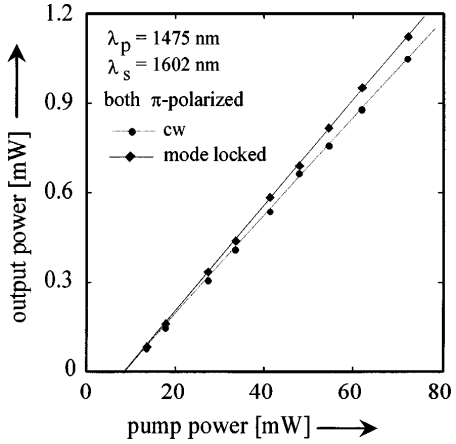


Fig. 2. Output power versus incident pump power of a diode-pumped ($\lambda_p \cong 1475$ nm) fiber-pigtailed and packaged Ti:Er:$LiNbO_3$ waveguide laser during cw and mode-locked operation. The pump and signal modes are $\pi$ polarized.

power characteristics are shown in Fig. 2. The slope efficiency during cw operation for the single-line ($\pi$-polarized) emission in the forward direction is ~1.6%. For this pump polarization, no additional emission line was observed to as high as the power limit of the pump laser diode. With $\sigma$- (TE-) polarized pumping, TM-polarized lasing at 1602 nm set in at a pump power level of 11 mW. Moreover, additional TE-polarized lasing at 1611 nm with $\cong$ 1.8% slope efficiency could be observed for pump power levels in excess of ~24 mW. Such dual-line output of orthogonal polarization can occur if the output at the wavelength of higher threshold has a higher slope efficiency.

To achieve mode-locked laser operation, we drove the phase modulator at the fundamental (1.282 GHz) and at harmonics of the axial-mode frequency spacing with as much as 31.5 dBm of incident rf power. The rf power reflection at the first, second, and third harmonics, measured with a network analyzer, is $< -10$ dB. Only for the fourth harmonic does the reflection reach $-6.1$ dB. The rf attenuation of the microstrip line (modulator electrodes) is $\simeq$2.3 dB for fundamental, 3.1 dB for second-harmonic and 6.4 dB for third-harmonic mode locking. The most stable mode locking is achieved at the third harmonic (3.823 GHz) because the length and the position of the phase-modulator electrodes are nearly optimized for this frequency.

An optical autocorrelator was set up to measure the width of the mode-locked pulses without the bandwidth limitations of direct detection. In the autocorrelator the incoming beam of pulses is split into two trains of variable mutual delay. These trains are correlated by use of noncollinearly phase-matched second-harmonic generation in a $LiNbO_3$ crystal, resulting in an offset-free correlation signal.

In addition to continuous mode locking, gain-switched mode-locked operation was investigated as a means of generating bursts of mode-locked pulses of higher peak power. During gain-switched operation the waveguide laser is pumped with square pulses of ~8-$\mu$s duration, 50% duty cycle, and 75-mW average power, leading to the emission of stable 2-$\mu$s-long (FWHM) laser pulses (first relaxation spike) of 7-mW peak power and 0.9-mW average power. By applying the rf drive voltage to the phase modulator, we generated mode-locked pulses of as much as 650-mW peak power, leading to 5.6 pJ of energy per pulse for the fundamental, 2.8 pJ for second-harmonic, and 2.4 pJ for third-harmonic mode locking. (The first figure already exceeds the pulse energy of 3.8 pJ reported for exciting a fundamental soliton of 6.4-ps width and 0.6-W peak power in a standard single-mode fiber at a 1.55-$\mu$m wavelength.[6]) Figure 3 shows autocorrelation traces for this mode of operation at the third

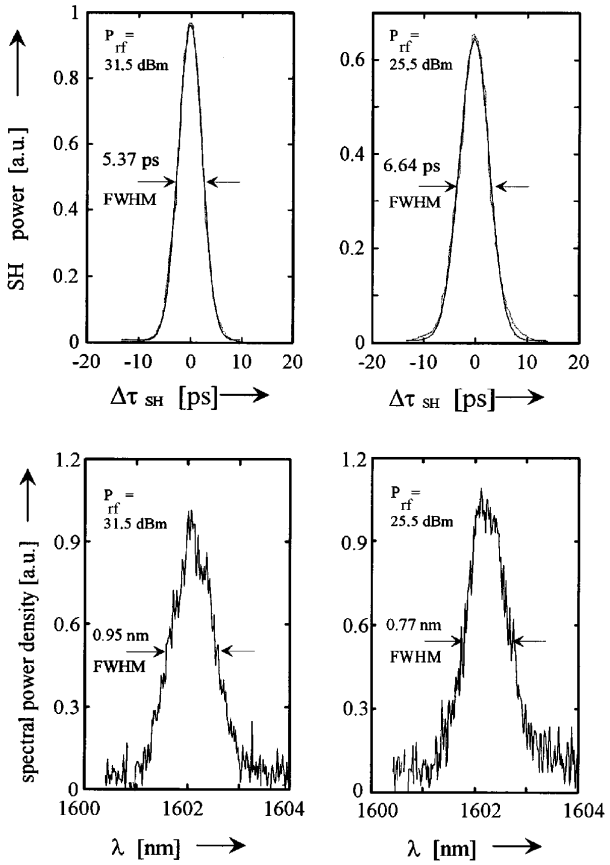


Fig. 3. Upper plots: pulse autocorrelation traces for third-harmonic mode locking (3.823-GHz pulse repetition frequency) plotted as second-harmonic (SH) power versus relative pulse delay. Lower plots: spectral power densities of the mode-locked laser emission versus wavelength. The parameter for all the graphs is the rf power level.

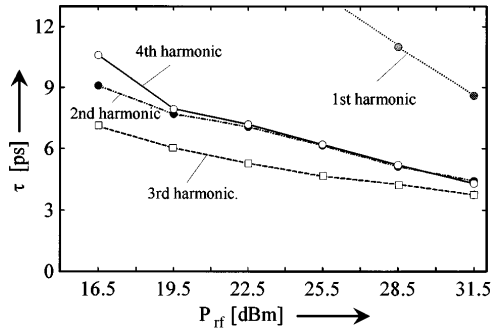


Fig. 4. Measured width (FWHM) of the mode-locked pulses versus incident rf power for various harmonics of the axial-mode frequency spacing.

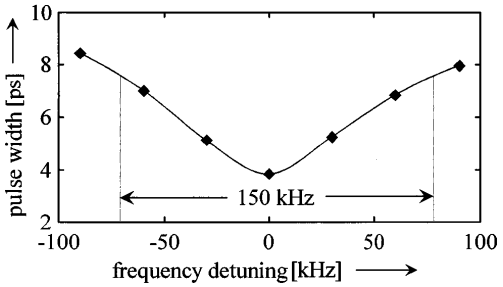


Fig. 5. Width (FWHM) of the mode-locked pulses for third-harmonic mode locking versus frequency detuning from the optimum locking condition. The incident pump power is ≅45 mW (five times the threshold pump power level).

harmonic and for two different parameters of the incident rf power level, together with the measured spectra. From the width (FWHM) of the autocorrelation trace at the maximum available rf power (31.5 dBm) and assuming a Gaussian pulse shape, a pulse width (FWHM) of ≅3.8 ps can be deconvolved, which fits well with the correlation traces. The corresponding pulse widths for fundamental, second-harmonic, and fourth-harmonic mode locking were 8.6, 4.4, and 4.3 ps, respectively. Using the width of the corresponding spectra (lower graphs of Fig. 3), we can calculate the pulse-width–bandwidth product. A figure of 0.42 was achieved for both rf power levels, in excellent agreement with the transform-limited product for Gaussian pulses. For FM mode locking this limit can be achieved only with a slight detuning from the axial-mode frequency spacing or harmonics thereof.[7]

The measured width of the mode-locked pulses for the four different harmonics as a function of the rf power level is shown in Fig. 4. As expected, the pulse widths decrease with increasing phase modulation index (rf power level).[7] The increase of the pulse width from the third to the fourth harmonic is due mainly to a worse impedance matching of the modulator (increased rf reflection) and a higher attenuation of the microwave along the modulator electrodes at the fourth harmonic. Even-shorter pulses can be expected at higher rf power levels and at higher harmonics of the axial mode spacing, provided that proper impedance matching and low rf attenuation along the traveling-wave modulator electrodes can be achieved.

Figure 5 shows the width of the mode-locked pulses as function of the frequency detuning from the optimum locking condition for third-harmonic mode locking and five times the threshold pump power level. Note that the pulse width doubles at approximately ±75-kHz detuning.

Another important feature is the temperature sensitivity of the locking frequency owing to changes of the optical path length in the cavity. The relative change of the locking frequency as a function of the temperature is $\sim 3.65 \times 10^{-5}/^{\circ}\mathrm{C}$, as expected from calculations based on published data of the thermal expansion and the temperature-dependent refractive index of $LiNbO_3$.[8]

In summary, mode locking has been achieved to as high as the fourth harmonic (5.124 GHz) of the axial-mode frequency spacing and is limited by our frequency generator. We are confident of achieving mode locking with even shorter pulses at higher harmonics. Such a mode-locked laser of multigigahertz pulse repetition frequency could be the key component of a transmitter unit for fast digital optical communications.

We gratefully acknowledge the support of this study by the European Union (Race-II project EDIOLL).

## References

1. I. Baumann, R. Brinkmann, Ch. Buchal, M. Dinand, M. Fleuster, H. Holzbrecher, W. Sohler, and H. Suche, in *Proceedings of European Conference on Integrated Optics* (CSEM, Neuchâtel, Switzerland, 1993), paper 3-14.
2. R. Brinkman, W. Sohler, and H. Suche, Electron. Lett. **27,** 415 (1991).
3. P. Becker, R. Brinkmann, M. Dinand, W. Sohler, and H. Suche, Appl. Phys. Lett. **61,** 1257 (1992).
4. H. Suche, I. Baumann, D. Hiller, and W. Sohler, Electron. Lett. **29,** 1111 (1993).
5. 1.48-$\mu$m pump source provided by Alcatel Alsthom Recherche; see R. Meilleur, A. Coquelin, R. M. Monnot, F. Brillouet, and E. Grard, in *Eleventh Annual Conference on European Fibre Optic Communications and Networks,* Proceedings Volume: Papers on Fibre Optic Communications (European Institute for Communications and Networks, Geneva, 1993), p. 205.
6. R. H. Stolen, L. F. Mollenauer, and W. J. Tomlinson, Opt. Lett. **8,** 186 (1983).
7. D. J. Kuizenga and A. E. Siegman, IEEE J. Quantum Electron. **QE-6,** 694 (1970).
8. G. J. Edwards and M. Lawrence, Opt. Quantum Electron. **16,** 373 (1984).